Luttinger Liquids

Nicholas T Brönn
Department of Physics
University of Illinois at Urbana-Champaign
1110 West Green Street
Urbana, Illinois 61801, USA

December 11, 2007

Abstract

The Fermi liquid theory of interacting electrons in one dimension breaks down due to the Peierls instability. Hence a different theory that takes into account explicitly the one-dimensional nature of the system must be found. This theory was pioneered by J.M. Luttinger, who was able to describe low-lying excitations in a one-dimensional electron gas in terms of bosons. Haldane completed the constructive approach to the theory and named it Luttinger liquid theory. More recently, advances in experimental techniques and the discovery of carbon nanotubes allowed effectively one-dimensional electron systems to be probed in the laboratory.

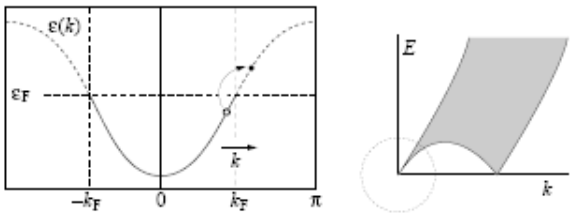

Figure 1: Particle-hole excitations in one dimension [1].

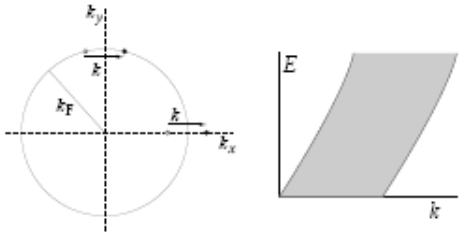

Figure 2: Particle-hole excitations in two dimensions[1].

1 Introduction

1.1 Inadequacy of Fermi Liquid Theory in One Dimension

In one dimension, the Fermi surface consists of just two points at $\pm k_F$. The fact that each branch of the Fermi surface can be mapped on the other by a single wavevector $\pm 2k_F$ produces a singular particle-hole response at $2k_F$ known as the Peierls instability. To see why this is a problem in one dimension, images of the Fermi surfaces and particle-hole excitations are depicted in Fig. 1 and Fig. 2 for one- and two-dimensions respectively. The constriction of the one-dimensional picture is responsible for the breakdown of Fermi liquid theory in one dimension. Note that in the two-dimensional picture, the allowed particle-hole excitations are "filled out."

1.2 History of Luttinger Liquid Theory

The history of Luttinger liquid theory actually goes back to the work of Tomonaga [2] from 1950, where he posited that excitations in one-dimensional systems could be described by a "quantized field of sound waves" or phonons. While this is true, it is more accurate to call these excitations plasmons after the work of Bohm and Pines (1953). Luttinger developed this theory into a model that he incorrectly solved in 1963 [3]. By failing to properly address the infite-dimensionality of the Hilbert space that changes the commutators of field

operators, he derived that the excitations were the same for interacting and non-interacting electron systems. Mattis and Lieb [4] fixed this problem in 1965, correctly writing down the field operators. Haldane [5] coined the term 'Luttinger liquid' (sometimes also called a 'Tomonanga-Luttinger liquiud') in 1981 and discovered a nice physical interpretation of what the bosonization of the one-dimensional fermion excitations means. The next section parallels the work of Eggert [6], which was derived from the work of Haldane.

2 Bosonization

2.1 Non-interacting system

Given c_k and $c_k^\dagger$ as the electron annihilation and creation operators respectively, the non-interacting Hamiltonian is given as

$$H = \sum_k \epsilon_k c_k^\dagger c_k,$$

where ϵ_k are the single-particle energies. The c_k and $c_k^\dagger$ obey the usual Fermi anti-commutation relations

$$\{c_k^\dagger, c_{k'}\} = \delta_{kk'} \qquad \{c_k, c_{k'}\} = \{c_k^\dagger, c_{k'}^\dagger\} = 0.$$

The field operators corresponding to these annihilation operators are given by the Fourier transform:

$$\psi(x_j) = \frac{1}{\sqrt{N}} \sum_{k=-\pi/a}^{\pi/a} e^{ikx_j} c_k \qquad c_k = \frac{1}{\sqrt{N}} \sum_{j=1}^{N} e^{-ikx_j} \psi(x_j),$$

where k is spaced in increments of $2\pi/Na$ and $x_j = ja$, a the lattice constant (also, $x_N = \ell$). The field operator corresponding to the creation operators is just the Hermitian conjugate of this. The $\psi(x_j)(\psi^\dagger(x_j))$ annihilate (create) a localized Wannier state at lattice site x_j.

2.2 Linearization of the Hamiltonian

The Fermi surface of a one-dimensional electron gas consists of two points, at $\pm k_F$. At absolute zero, every state between these two wavevectors is occupied. Around the Fermi surface, we may separate the electrons into right-movers, with $k \approx k_F$, and left-movers, with $k \approx -k_F$, and linearize their energies as

$$\epsilon_k \approx \epsilon_F + (k - k_F) \frac{\partial \epsilon_k}{\partial k}\bigg|_{k=k_F} + O((k-k_F)^2) \approx v_F(k - k_F) \qquad \text{for} \qquad k \approx k_F$$

for the right-movers and

$$\epsilon_k \approx \epsilon_F + (k + k_F) \frac{\partial \epsilon_k}{\partial k}\bigg|_{k=-k_F} + O((k+k_F)^2) \approx -v_F(k + k_F) \qquad \text{for} \qquad k \approx -k_F$$

for the left-movers, where we take the Fermi energy to be zero. Define Λ as the range of validity for this linearization approximation as in Fig. 3, so that the linearized effective

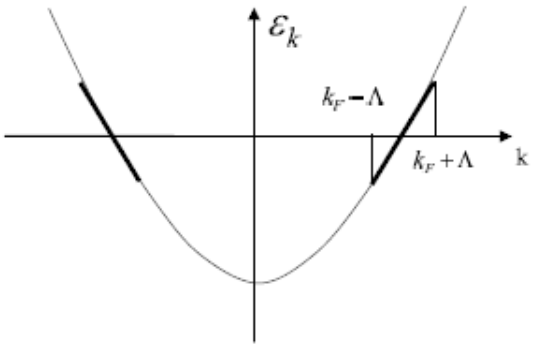

Figure 3: The linear region of the band.

Hamiltonian is

$$H \approx \sum_{k=k_F-\Lambda}^{k_F+\Lambda} \epsilon_k c_k^\dagger c_k + \sum_{k=-k_F-\Lambda}^{-k_F+\Lambda} \epsilon_k c_k^\dagger c_k$$

This expression may be made more concise if we define new quantum operators

$$c_k^R = c_{k_F+k} \qquad c_k^L = c_{-k_F+k}$$

for $|k| < \Lambda$ as right- and left-moving annihilation operators by shifting the original ones relative to the Fermi wavevector points. Then the linearized Hamiltonian may be written as

$$H = \sum_{k=-\Lambda}^{\Lambda} v_F k (c_k^{R\dagger} c_k^R - c_k^{L\dagger} c_k^L).$$

We also find that the original fermion field operator splits into right- and left-moving parts:

$$\begin{aligned}
\psi(x_j) &= \frac{1}{\sqrt{N}} \sum_k e^{ikx_j} c_k \\
&= \frac{1}{\sqrt{N}} \left(\sum_{k=k_F-\Lambda}^{k_F+\Lambda} + \sum_{k=-k_F-\Lambda}^{-k_F+\Lambda} \right) e^{ikx_j} c_k \\
&= \frac{1}{\sqrt{N}} \left(e^{ik_F x_j} \sum_k e^{ikx_j} c_k^R + e^{-ik_F x_j} \sum_k e^{ikx_j} c_k^L \right) \\
&= \sqrt{a} (e^{ik_F x_j} \psi^R(x_j) + e^{-ik_F x_j} \psi^L(x_j)),
\end{aligned}$$

where we have defined

$$\psi_R(x_j) = \frac{1}{\sqrt{\ell}} \sum_k e^{ikx_j} c_k^R \qquad \psi_L(x_j) = \frac{1}{\sqrt{\ell}} \sum_k e^{ikx_j} c_k^L.$$

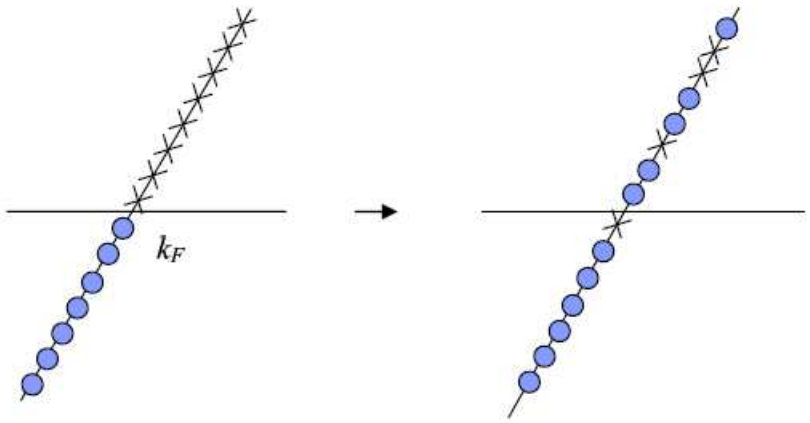

Figure 4: Particle-hole excitations

We have not explicitly labelled the range of summation in this expression for a reason. Although we have explicitly introduced a cut-off because we only care about low-lying excitations, we can include all the states $-\infty < k < \infty$ explicity because we will always limit ourselves to low-level excitations, hence the added states outside the cut-off will never contribute to any physical excitation. Primarily we do this so that the Fourier transform of the right- and left-moving field operators may be represented by the continuous integral

$$c_k^{R/L} = \frac{1}{\sqrt{\ell}} \int_0^\ell e^{-ikx} \psi_{R/L}(x)\, dx.$$

It should also be noted that by including all these state, the anti-commutator

$$\left\{ \psi_{R/L}^\dagger(x), \psi_{R/L}(y) \right\} = \delta(x-y)$$

is normalized as a delta function as opposed to being dependent on the cut-off Λ.

2.3 Excitation Spectrum

In this section we will show how excitations of a one-dimensional Fermi gas at absolute zero may be thought of as bosonic occupation numbers. This will be done by construction of the excited state in Fig. 4. First, we consider only right-moving electrons, and temporarily drop the superscript R on the operators. For simplicity we replace the subscript on the creation/annihilation operators by excitation mode, i.e. c_0 corresponds to annihilating the electron at $k = k_F$, $c_1^\dagger$ corresponds to creating an electron in the 1st excited state, such that the state created in Fig. is described by

$$c_0 c_1^\dagger c_2^\dagger c_4^\dagger c_5^\dagger c_8^\dagger |0\rangle,$$

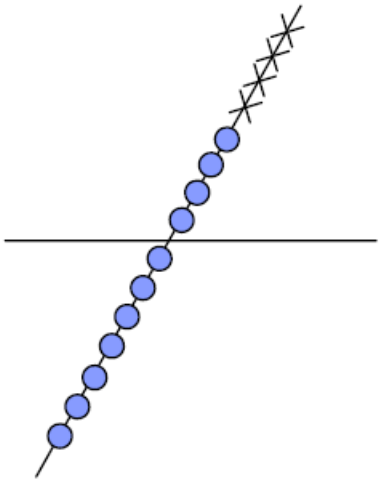

Figure 5: Step one of the bosonization example is to add 4 electrons.

where $|0\rangle$ is the ground state of the filled Fermi sea. Since the order of operators is important, we write the operators from left to right corresponding to lowest to highest integer. Instead of doing this all at once, we break down this process into steps:
Step 1: Create the excited state in Fig. 5 by operating

$$c_1^\dagger c_2^\dagger c_3^\dagger c_4^\dagger |0\rangle$$

on the filled Fermi sea. The energy cost of this is

$$E = \frac{\pi v_F}{N} n_R^2,$$

where n_R is the number of right-movers added.

Step 2: Now we shift each of these excitations, starting from the highest to lowest, in order to create particle-hole excitations:

- shift the electron at $n = 4$ up 4 steps to level 8, with an energy cost of $E = 1 \times 4 \times 2\pi v_F/N$
- shift no electrons up 3 steps
- shift the next two electrons, at $n = 3, 2$ respectively, up 2 steps to levels $5, 4$, with an energy cost of $E = 2 \times 2 \times 2\pi v_F/N$
- shift the next two electrons, at $n = 1, 0$ respectively, up 1 step to levels $2, 1$, with an energy cost of $E = 2 \times 1 \times 2\pi v_F/N$

In this step we created the resultant state in Fig. 4

Step 3: Associate each shift of Step 2 with a boson of the same energy, as in

- one excited boson on level 4
- no excited bosons on level 3
- two excited bosons on level 2
- two excited bosons on level 1

In this way we can represent particle-hole excitations as bosons. This will be made more rigorous in the next subsection.

2.4 Boson operators

We will now define some boson operators and state some relations between them so that we may write our old fermion operators in terms of these. In order to limit the amount of tediousness in this section, the reader is referred to Ref for derivations of many of these results.

First we define the fermion shifting operators as

$$\rho_k^R = \sum_{k'} c_{k'+k}^{R\dagger} c_{k'}^R,$$

which can be seen as shifting all the right-movers up by an amount k. Since we include all states below k_F, this creates an analogous situation to Step 1 in the subsection above. Notice that the fermion shifting operator is not Hermitian, indeed $(\rho_k^R)^\dagger = \rho_{-k}^R$, meaning that the Hermitian conjugate will "annihilate" an excitation by amount k, which should be expected for bosonic operators. Also consider the commutator

$$[(\rho_k^R)^\dagger, \rho_{k'}^R] = [\rho_{-k}^R, \rho_{k'}^R] = \delta_{kk'} \frac{kN}{2\pi},$$

where care must be taken in deriving the result for $k = k'$ due to the infinity of states in the Fermi sea. This result, along with the commutator of the shifting operator with the Hamiltonian,

$$[H, \rho_k^R] = \sum_{k',k''} v_F k' [c_{k'}^{R\dagger}, c_{k'}^R, c_{k''+k}^{R\dagger} c_{k''}^R] = v_F k \rho_k^R,$$

gives us the boson algebra and the Hamiltonian in terms of boson operators. We rescale the shifting operators as

$$b_k^{R\dagger} = i\sqrt{\frac{2\pi}{kN}} \rho_k^R \qquad b_k^R = -i\sqrt{\frac{2\pi}{kN}} \rho_{-k}^R,$$

and since for left-movers the excitations correspond to $k < 0$,

$$b_k^{L\dagger} = -i\sqrt{\frac{2\pi}{kN}} \rho_{-k}^L \qquad b_k^L = i\sqrt{\frac{2\pi}{kN}} \rho_k^R.$$

This gives us the canonical boson commutation relations

$$[b_k^R, b_{k'}^{R\dagger}] = \delta_{kk'} \qquad [H, b_k^{R\dagger}] = v_F k b_k^{R\dagger},$$

from which we may build up the spectrum, and write the Hamiltonian as

$$H = \sum_{k>0} v_F k \left(b_k^{R\dagger} b_k^R + b_k^{L\dagger} b_k^L \right) + \frac{\pi v_F}{N} (n_R^2 + n_L^2).$$

Here the second term corresponds to the initial addition of electrons, as in our constructed example, called the *zero modes*. The terms in the sums correspond to particle-hole excitations are called the *oscillation modes*.

2.5 Fermion operators expressed as boson operators

Using our right- and left-moving fermion fields, we can construct right- and left-moving fermion densities given by

$$\rho_{R/L}(x) = \psi_{R/L}^\dagger(x) \psi_{R/L}(x),$$

which will turn out to be related to the fermion shifting operators. However, before we continue, we must note that for the ground state,

$$\langle \rho_R(x) \rangle = \sum_{kk'} e^{-ikx} e^{ik'x} \langle c_k^{R\dagger} c_k^R \rangle = \sum_{k=-\infty}^{0} \langle c_k^{R\dagger} c_k^R \rangle = \infty,$$

that is, there are an infinite number of electrons in our Fermi sea. We can solve this problem by *normal ordering*, in which we rearrange our operators to subtract off the ground state expectation value,

$$: \rho_R(x) := \psi_R^\dagger(x) \psi_R(x) - \langle \rho_R(x) \rangle.$$

This is accomplished by moving our fermion annihilation operators to the right for $k > 0$ and to the left for $k \leq 0$, as in

$$: c_k^{R\dagger} c_k^R := - : c_k^R c_k^{R\dagger} := \begin{cases} c_k^{R\dagger} c_k^R & k > 0 \\ -c_k^R c_k^{R\dagger} & k \leq 0 \end{cases}.$$

With this in mind, we can now calculate the Fourier transform of the right-moving fermion densities

$$\int_0^\ell dx\, e^{ikx} : \rho_R(x) := \sum_{k'} : c_{k'+k}^{R\dagger} c_{k'}^R := \begin{cases} \rho_k^R & k \neq 0 \\ n_R & k = 0 \end{cases},$$

which is just the fermion shifting operators for the oscillating modes or number of right-movers added for the zero mode. By taking the inverse Fourier transform, we have expressions for the fermion densities in terms of boson operators:

$$: \rho_R(x) := \frac{1}{\ell} \sum_{n=1}^{\infty} \sqrt{n} \left(i b_n^R e^{i \frac{2\pi}{\ell} nx} - i b_n^{R\dagger} e^{-i \frac{2\pi}{\ell} nx} \right) + \frac{n_R}{\ell},$$

and similarly for the left-movers, but the R is switched with L and the signs in the exponentials are opposite. If now we define the boson field operators as

$$\phi_R(x) = \phi_0^R + Q_R \frac{x}{\ell} + \sum_{n=1}^{\infty} \frac{1}{\sqrt{4\pi n}} \left(e^{i \frac{2\pi n}{\ell} x} b_n^R + e^{-i \frac{2\pi n}{\ell} x} b_n^{R\dagger} \right)$$

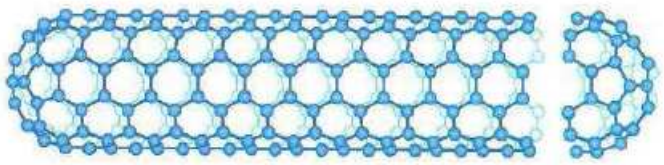

Figure 6: Model of a single-walled carbon nanotube [6].

and simlarly for the left-moving boson field (with R replaced with L and opposite signs in the exponentials), then we may write

$$: \rho_{R/L}(x) := \frac{1}{\sqrt{\pi}} \partial_x \phi_{R/L}(x),$$

where $Q_{R/L} = \sqrt{\pi} n_{R/L}$ and $\phi_0^{R/L}$ are defined as conjugate to the number operators

$$[\phi_0^R, Q_R] = -i/2 \qquad [\phi_0^L, Q_L] = i/2.$$

We can also express the Hamiltonian in terms of boson fields as

$$H = a v_F \int_0^\ell dx \, ((\partial_x \phi_R(x))^2 + (\partial_x \phi_L(x))^2).$$

3 Experimental Results in Carbon Nanotubes

3.1 Overview

Carbon nanotubes (Fig. 6) are tightly rolled up sheets of graphene, a hexagonal sheet of carbon atoms. Single-walled carbon nanotubes are typically about 0.5-2.0nm in diameter, thus thin enough that the excitations in the circumferential direction are frozen out, and we have an effective one-dimensional electron gas. It has also been shown [8] that the instability caused by the lattice distortion when a carbon nanotube "bends" is not important.

All of the results verifying Luttinger liquid behavior in carbon nanotubes has thus far been about the measurement of anomalous critial exponents, as found in the last section. For example, near the Fermi surface, the density of states [6]

$$\rho(\omega) \propto |\omega|^\alpha \qquad \alpha = \frac{1}{4}(g + g^{-1} - 2) > 0,$$

where g is the one-dimenstional electron-electron interaction parameter. In the case of nanotubes contacted to metallic tunelling leads, in the case of small bias voltages $V \ll k_B T/e$, there is a power-law variation of conductance with temperature [9]

$$G \propto T^\alpha,$$

Figure 7: A bundle of single-walled carbon nanotubes observed via tunelling electron microscopy [8].

and for high bias voltages $V \gg k_B T/e$ there is a power-law variation of (differential) conductance with bias voltage

$$dI/dV \propto V^{\alpha},$$

where α depends on whether the nanotube was contacted to its bulk or end as

$$\alpha = \begin{cases} \frac{1}{8}(g + g^{-1} - 2) & \text{bulk} \\ \frac{1}{4}(g^{-1} - 1) & \text{end} \end{cases}.$$

3.2 Photoemission Spectroscopy

In this experiment, Ishii et. al. [8], measured the photoemission spectra from a synchrotron source of ropes of carbon nanotubes grown by laser ablation. A bundle of these ropes is shown in Fig. 7 These carbon nanotubes were determined to have apporximately the same diameter. The results for observed photoemission spectra and calculated photoemission and density-of-state data for the Tomonaga-Luttinger-Liquid model is given in Fig. 8

3.3 Electron Transport

In another experiment, Bockrath et. al. [9], measured the anomalous Luttinger liquid critial exponents for how conductivity in a single-walled carbon nanotube scales with temperature and bias voltage. The nanotubes were contacted using two different methods. The leads were defined via electron-beam lithography either before or after the deposition of nanotubes from a dichloroethane solution. Hence the chromium/gold leads may be on top or on bottom of the nanotubes. Only nanotubes with well-defined periodic Coloumb blockade at low-temperatures were used because this indicated the presence of a single *quantum dot* [9].

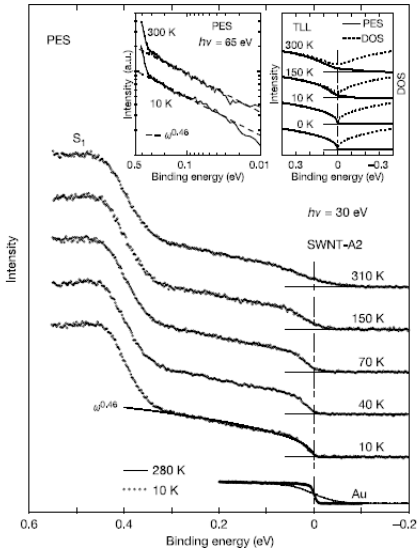

Figure 8: Observed and calculated photoemission spectra and density-of-states. The exponent determined here is $\omega = 0.46$ [8].

In Fig. 9 the conductance versus bias voltage it shown. The conductance is scaled by a temperature-dependent prefactor, based on theory, so that curves at different temperatures can be compared. The power law is readily evident from this log-log plot.

References

[1] D Senechal, An introduction to bosonization, arXiv:cond-mat/9908262v1 (1999)

[2] S Tomonaga, Remarks on Bloch's Method of Sounds Waves applied to Many-Fermion Problems, *Prog Theor Phys* **5**, 4 (1950)

[3] JM Luttinger, An exactly soluable model of a many-fermion system, *J Math Phys* **4**, 9 (1963)

[4] DC Mattis, EH Lieb, Exact Solution of a Many-Fermion System and Its Associated Boson Field, *J Math Phys* **6**, 2 (1965)

[5] FDM Haldane, 'Luttinger liquid theory' of one-dimension quantum fluids: I. Properties of the Luttinger model and their extension to the general 1D interacting spinless Fermi gas, *J Phys C: Solid State Phys* **14**, 2585 (1981)

[6] S Eggert, A pedestrian approach to bosonization, arXiv:cond-mat/0807.0003v2 (2007)

[7] F Anfuso and S Eggert, Luttinger liquid in a finite one-dimensional wire with box-like boundary conditions, *Phys Rev B* **68** 241301(R) (2003)

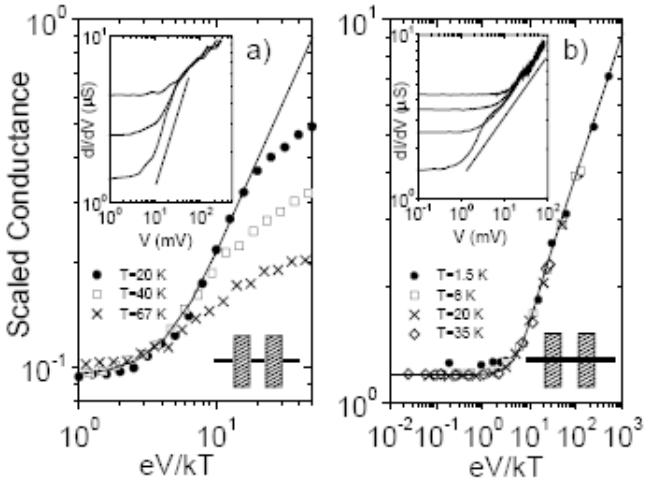

Figure 9: Differential conductance scaled by temperature vs bias voltage. In (a) the nanotubes are contacted in the bulk with $\alpha = 0.36$ and (b) the nanotubes are contacted on the ends with $\alpha = 0.87$ [9].

[8] H Ishii, H Kataura, H Shiozawa, H Yoshioka, H Otsubo, Y Takayama, T Miyahara, S Suzuki, Y Achiba, M Nakatake, T Narimura, M Higashiguchi, K Shimada, H Namatame, M Taniguchi, Direct observation of Tomonaga-Luttinger-liquid state in carbon nanotubes at low temperatures, *Nature*, **426**, 540 (2003)

[9] M Bockrath, DH Cobden, J Lu, AG Rinzler, RE Smalley, L Balents, PL McEuen, Luttiner Liquid Behavior in Carbon Nanotubes, *Nature* **397**, 598 (1999)